ANALYSIS OF THE HYDRODYNAMICS AND HEAT TRANSFER ASPECTS OF MICROGRAVITY TWO-PHASE FLOWS

Kamiel S. Rezkallah
Department of Mechanical Engineering
University of Saskatchewan
Saskatoon, SK S7N 5A9
CANADA

ABSTRACT

Experimental results for void fractions, flow regimes and heat transfer rates in two-phase, liquid-gas flows are summarized in this paper. The data was collected on-board NASA's KC-135 reduced gravity aircraft in a 9.525 mm circular tube (i.d.), uniformly heated at the outer surface. Water and air flows were examined as well as three glycerol/water solutions and air. Results are reported for the water-air data.

INTRODUCTION

Two-phase thermal transport systems have been utilized and researched in the nuclear and petrochemical industries for many decades. Despite the numerous efforts (experimentally, analytically and numerically), two-phase flow models still lack essential information on the interface dynamics and flow characteristics to provide for closure solutions. The microgravity environment provides a good tool to examine the flow without the masking effects of gravitational forces on ground. Flow regimes are basically divided into three regions, namely surface tension dominated region (bubbly and slug flows), inertia dominated region (annular flow) where minimum differences exist between 1-g and μ-g , and an intermittent region (which is mostly occupied by a frothy slug-annular flow). These regions are shown in Figure 1 on a map with dimensionless coordinates in terms of the phase Weber number.

While there is a substantially large body of information on two-phase, gas-liquid flows at 1-g (both adiabatic and in boiling/condensing systems), the knowledge-base for their use in space hardware has only recently been growing. Early experimental studies of two-phase convective heat transfer under microgravity conditions were reported by Papell [1] and Feldmanis [2]. In the first study, Papell [1] reported a 15% increase in the heat transfer rate for a sub-cooled water system during reduced gravity. Feldmanis [2], on the other hand, did not explicitly determine heat transfer coefficients. Instead, based on the temperature measurements made during his experiment, he predicted that for forced convective condensation gravity would have little influence on heat transfer.

More recently, Reinharts, Best and Hill [3] worked with a boiling and condensing Refrigerant-12 test loop on-board NASA's KC-135. They reported that the condensation heat transfer coefficients were 26% lower for μ-g conditions as opposed to 1-g condition. Boiler temperatures remained constant throughout the KC-135 flights. Thus, no conclusions could be drawn on the effect of gravitational acceleration on the boiling heat transfer coefficients. Ohta et al. [4] completed a study of convective boiling system with Refrigerant-113 flow through a 8 mm ID circular tube. They reported that while boiling was occurring in the bubbly and annular flow regimes, there was no difference in the heat transfer coefficients between 1-g and μ-g conditions. However, when boiling was suppressed due to the high flow rates and low heat flux, the heat transfer coefficients were lower at μ-G compared with 1-g. With such conflicting results, it is clear that further experimental investigation into the heat transfer behavior of two-phase flows under μ-g is warranted.

SYMBOLS

A	annular flow regime		V_{SG}	superficial gas velocity, m/s
B	bubbly flow regime		x	gas quality
g	earth's gravitational acceleration			
h	heat transfer coefficient, $W/m^2.K$		*Greek Symbols:*	
Nu	Nusselt number (dimensionless)			
PDF	Probability Density Function		α	gas void fraction (volumetric)
S	slug flow regime		μ	"micro"
V_{SL}	superficial liquid velocity, m/s			

TEST APPARATUS AND PROCEDURE

A forced-convective two-phase test apparatus was designed and built for testing aboard NASA's KC-135 Zero-G aircraft. The apparatus is instrumented such that simultaneous measurements of pressure drop, void-fraction and heat transfer data can be made, with continuous observation and recording of the two-phase flow patterns. In order to cover a wide range of test conditions, the facility allows for the independent control of three separate parameters during testing: air flow rate, water flow rate, and temperatures of the two-phase mixture in the flow loop. A schematic of the test apparatus is shown in Figure 2.

On-board the plane the apparatus was situated such that the observation and heated test sections were oriented vertically with respect to the floor of the aircraft. A complete discussion of the flow loop may be found in Rite and Rezkallah [5]. Data were mostly gathered for air-water mixtures. In addition, data were also collected with three air-glycerol/water solutions of 50%, 59%, and 65% glycerol (by weight), respectively. These mixtures were used to examine the effect of changing the liquid viscosity on the heat transfer rates and flow transitions/pressure drops. The data were also used in the development of a set of empirical heat transfer correlations.

Quasi-steady-state conditions were obtained during the short μ-g duration. This was investigated experimentally, first on-ground and later during flight. It was determined that in a worst case scenario, after approximately ten seconds quasi-steady-state conditions were achieved for all flow rates. It was decided therefore that data for only the last ten seconds of each parabola would be included in the average heat-transfer values. More complete details on the above mentioned tests can be found in Rite and Rezkallah [6,7]. In addition, an analytical study by Zhao and Rezkallah [8] confirmed these results.

EXPERIMENTAL RESULTS

Average Heat Transfer Coefficients

Sample results are shown in Figures 3(a) and 3(b) for the two-phase flow Nusselt numbers versus the gas quality, x. The superficial liquid velocity "V_{SL}" ranged from 0.07 to 2.5 m/s. The flow regime for each data point is also marked besides each point. The abbreviations for the various flow regimes are as follows: "B" for bubbly, "S" for slug, and "A" for annular flow.

It can be seen that at low gas qualities (mainly in the bubbly and slug flow regions), the 1-g Nusselt number values are much greater than those measured at μ-g for the same liquid flow rates. As the gas flow rate increases (thus moving to annular flow conditions with high gas inertia), the 1-g and μ-g data points approach one another. This suggests that the difference between 1-g and μ-g behavior is flow regime dependent. Complete results for all fluids tested are given in Rite [9].

Local Heat Transfer Coefficients

The results of the local heat-transfer coefficients are shown in Figures 4(a) and 4(b). In these figures, the local heat transfer coefficients, h_{local}, were calculated from each of the 12 surface measurements on the heated test section using the following equation:

$$h_i = \frac{E}{\pi LD\,(T_{s,i} - T_{b,i})} \tag{1}$$

where E is the total heat input into the test section (W), L is the length of the heated test section (m), and $T_{b,i}$ is the average bulk fluid temperature at the i-th section of the heated tube (^{o}C). Integration with respect to length then provided an average heat transfer coefficient (h_{TP}).

Figures 4(a) and 4(b) show the local heat transfer measurements at a constant liquid superficial velocity V_{SL} of 0.10 m/s ($Re_{SL} \approx 1200$). In these figures, slug flow is present at each gas velocity, and the 1-g data shows an increase in the local heat transfer coefficient from inlet to exit, while the μ-g results show a decrease in h_{local} similar to what is commonly seen with single-phase

flows in the viscous flow region. The local minima and maxima in the local heat transfer coefficient, shown in the figures at locations 2&10, are in fact due to overlap in the heater wire at those locations.

The 1-g results described above for slug flow agree well with the findings of Vijay, Savic, and Sims [10]. They hypothesized that the effect of buoyancy forces on the gas bubbles caused the gas to have a greater velocity than the surrounding liquid. This "slip" between the phases led to a break-down in the laminar sub-layer near the tube wall, thus leading to a movement away from laminar flow-type behavior (i.e., a relatively long thermal entry length). However, under μ-g conditions this does not happen. The reduction of gravity greatly lessens the buoyancy forces and therefore the turbulence-generating ability of the gas bubbles; Elkow & Rezkallah [11]. The bubble movement at μ-g do not largely interfere with the maintenance of the laminar sub-layer. Further analysis based on the flow regime associated with the flow were made, and results can be found in Rite [9].

VOID-FRACTION RESULTS

Void fraction measurements ranging from approximately 0.1 to 0.9, and covering flow regimes from bubbly to annular flow were simultaneously obtained during flight testing. The results for slug flow are presented here. Complete results over the entire range of flow regimes can be found in Elkow [12]. In a comparison of the overall average void fraction values, it was found that small differences exist between the 1-g and μ-g cases only for bubble and slug flows. The overall average void fraction for slug flow was approximately 10% higher at μ-g conditions when compared to 1-g. However, instead of only considering the average values, the temporal fluctuations were analyzed with the use of Probability Density Function (PDF) plots.

Slug Flow Results

The PDF plots are shown for slug flow in Figures 5(a) and 5(b)for μ-g and 1-g, respectively. For these figures, the flow rates were V_{SL} = 0.24 m/s and V_{SG} = 0.19 m/s. The PDF plots show that there is a greater fluctuation in void fraction at 1-g. For this type of flow, the predominant forces include those due to buoyancy, surface tension, and turbulent stresses. At 1-g, forces due to gravitational acceleration tend to accelerate the bubbles and hence increase the probability of their interactions and coalescence.

Slug flow is characterized by the presence of "bullet shaped" bubbles, commonly known as Taylor bubbles. Due to buoyancy effects at 1-g, smaller bubbles will eventually "catch-up" with the Taylor bubble and hence increase α. An additional factor at 1-g is due to slip. Since there is a relative velocity between the liquid and gas phases, a low pressure region in the wake of the Taylor bubble exists. Therefore, smaller bubbles are drawn into the trailing end of the Taylor bubble, causing coalescence to occur due to the high turbulent mixing. Thus, at 1-g, as shown in Figure 5(a), fluctuations can be seen from α=0.0 to approximately 0.75. With buoyancy negligible at μ-g, turbulence is lower, resulting in a more structured flow. For this case the void fraction fluctuations were between α = 0.3 to 0.55.

Further discussion and interpretation of the PDF results can be made based on the flow images shown in Figures 6(a) and 6(b). Taylor bubble like flows at μ-g are more uniform in length (Figure 6b). The Taylor bubbles at μ-g vary from only 1 to 3 tube diameters, whereas at 1-g the Taylor bubble for the same flow rates ranges from 1 to 6 tube diameters. Further evidence of the effects of buoyancy can be seen in the flatter trailing end of the Taylor bubble at 1-g (Figure 6a), whereas the trailing end of the Taylor bubble at μ-g (shown in Figure 6b) where buoyancy is negligible, is seen to be more rounded.

Buoyancy causes a relative velocity difference between the liquid and gas phases. With the gas phase having the higher velocity, a low pressure region at the tail of the Taylor bubble would occur. From the video recordings in this region, it has been observed that coalescence is enhanced when another Taylor bubble approaches this low pressure region. However, at μ-g there is essentially no slip, thus a low pressure region at the tail of a Taylor bubble does not exist. It has been observed from video recordings that Taylor bubbles within close proximity to each other rarely coalesce at μ-g.

Heat transfer measurements in slug flow, shown earlier in Figure 3(a), indicate that the heat transfer coefficients at 1-g can be 28 to 40% higher than their counterparts at μ-g (corresponding to

a void fraction increase from approximately 0.3 to 0.65). This could be perhaps explained in terms of the results shown in Figures 6(a)&(b). The wider fluctuations at 1-g enhance mixing due to the greater turbulence, resulting in higher heat transfer coefficients.

SUMMARY AND CONCLUSIONS

It was found that for low liquid flow rates reduced gravity retards the heat transfer coefficient by up to 50% at the lowest gas qualities (bubbly and slug flow regimes). As the gas quality is increased (transition to annular flow), the difference between the 1-g and μ-g heat transfer coefficients becomes smaller. At higher liquid velocities, an increase in the gas quality results in the μ-g heat transfer coefficients being greater than those at 1-g by approximately 10%, which is within the uncertainty of the measurements. The influence of gravity was found to be both a single-phase effect and a two-phase effect. Mixed convection in the liquid phase affects the heat transfer coefficients, and reduced gravity has a substantial influence on the interfacial surface between the two phases.

Using a capacitance void fraction sensor, volumetric void fraction measurements were obtained for adiabatic two-phase, water-air flows at 1-g and μ-g. Comparisons of the void fraction signals at both gravity levels were made using PDF plots. It was found that a greater fluctuation in void fraction for slug flow existed at 1-g. At ground conditions fluctuations were in the range, $0 < \alpha < 0.75$, while at μ-g the fluctuations were within a much narrower range; $0.3 < \alpha < 0.55$. The PDF histograms for annular flow were found to be similar for both 1-g and μ-g flows. A very narrow fluctuation from approximately $0.8 < \alpha < 0.9$ was observed. This is expected since the flow in this regime is highly inertia dominated.

Acknowledgments

REFERENCES

[1] Papell, S.S. (1962) An instability effect on two-phase heat transfer for subcooled water flowing under conditions of zero gravity *American Rocket Society 17th Annual Meeting and Space Flight Exposition.*

[2] Feldmanis, C.J. (1966) Pressure and temperature changes in closed loop forced convection boiling and condensing processes under zero gravity conditions *Institute of Environmental Sciences' 1966 Annual Technical Meeting Proceedings.*

[3] Reinarts, T., Best, F.R., and Hill, W.S. (1992) Definition of condensation two-phase flow behaviors for spacecraft design *AIP Conference Proc.* , Vol. 246, pp.1216-1225.

[4] Ohta et al.(1994) Microgravity flow boiling in a transparent tube *10th International Heat Transfer Conference,* Brighton, England, No. 111.

[5] Rite, R.W., and Rezkallah, K.S. (1993) An investigation of transient effects on heat transfer measurements in two-phase gas-liquid flows under microgravity conditions *ASME Heat Transfer in Microgravity Systems - 1993,* pp. 49-57.

[6] Rite, R.W. and Rezkallah, K.S. (1994a) Heat transfer in two-phase flow through a circular tube at reduced gravity *Journal of Thermophysics and Heat Transfer* , Vol. 8, No. 4, pp. 702-708.

[7] Rite, R.W., and Rezkallah, K.S. (1994b) The influence of liquid viscosity on heat transfer coefficients in gas-liquid flows under microgravity conditions *AIP Conference Proc.,* Vol. 301, pp. 1129-1136.

[8] Zhao, L. and Rezkallah, K.S. (1993) The transient effects on the two-phase flow heat transfer at microgravity, *29th National Heat Transfer Conference,* Paper No. 93-3905, Atlanta, GA.

[9]Rite, R.W. (1995) *Heat Transfer in Gas-Liquid Flows through a Vertical, Circular Tube under Microgravity Conditions,* Ph.D. Thesis, Saskatoon: University of Saskatchewan.

[10] Vijay, M. M., Savic, P., and Sims, G. E., 1978, "The Graetz Problem for Two-Phase Two-Component Gas-Liquid Flow in Vertical Tubes," *Proc. 6th Int. Heat Transfer Conf.,* Vol. 1, pp. 493-497.

[11]Elkow, K.J., 1995, "Void-Fraction Measurements and Analysis at Normal and Microgravity Conditions, M.Sc. Thesis, University of saskatchewan, saskatoon, Canada.

[12]Elkow, K.J., and Rezkallah, K.S., 1996, " Void-Fraction Measurements in Gas-Liquid Flows Using capacitance Sensors, J. Measurement Science & Technology, (in press).
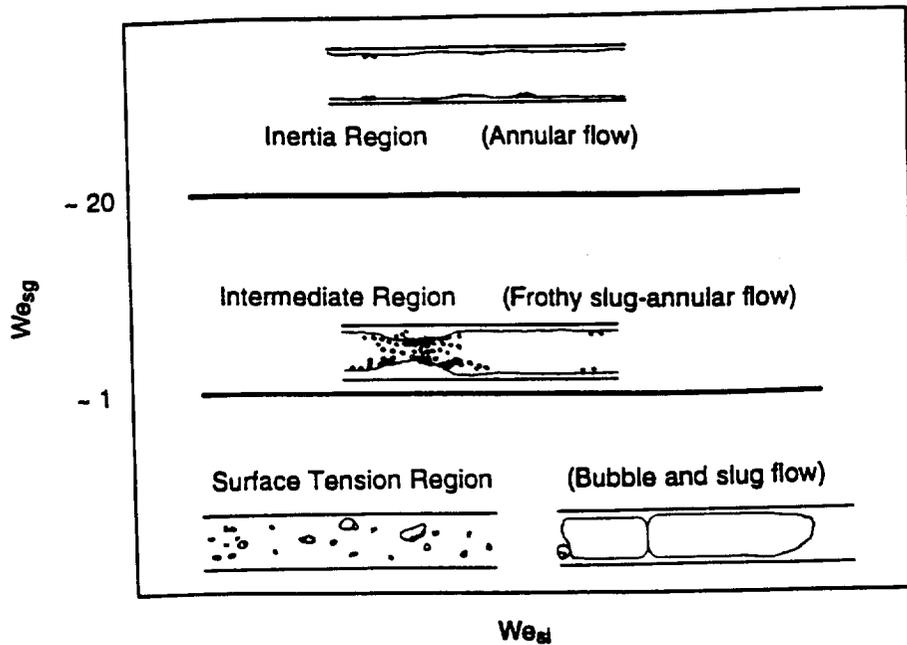
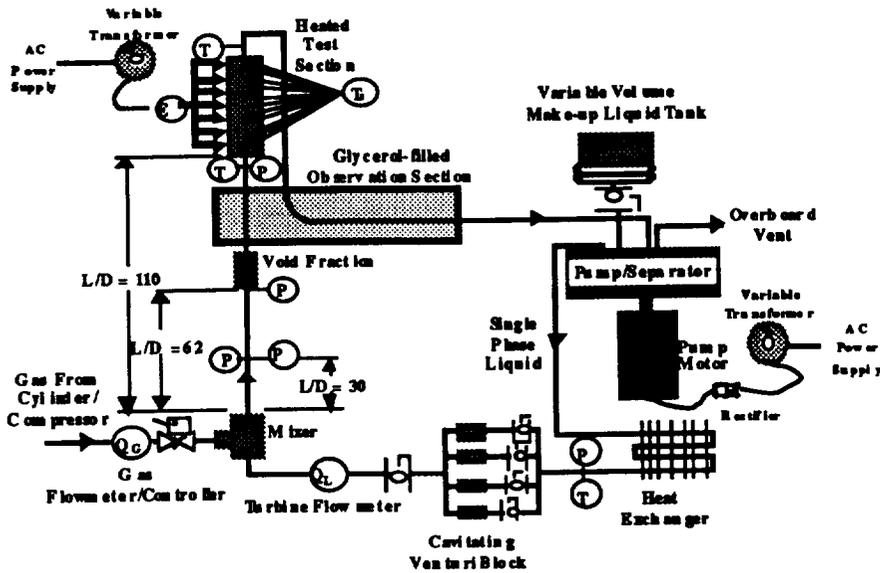**Figure 1. Weber Number based Flow Pattern Map for Two-Phase Flows at Microgravity**

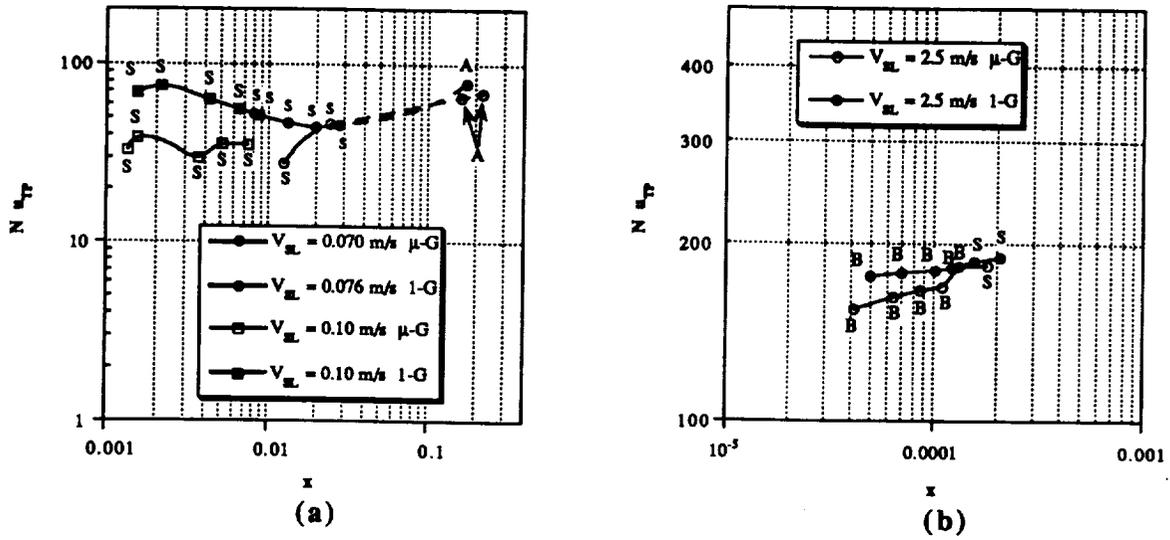**Figure 2. A Schematic of the Two-Phase Flow Loop**

Figure 3. Mean Heat Transfer Results at Microgravity; (a) Vsl=0.07&0.1 m/s, (b) Vsl=2.5 m/s

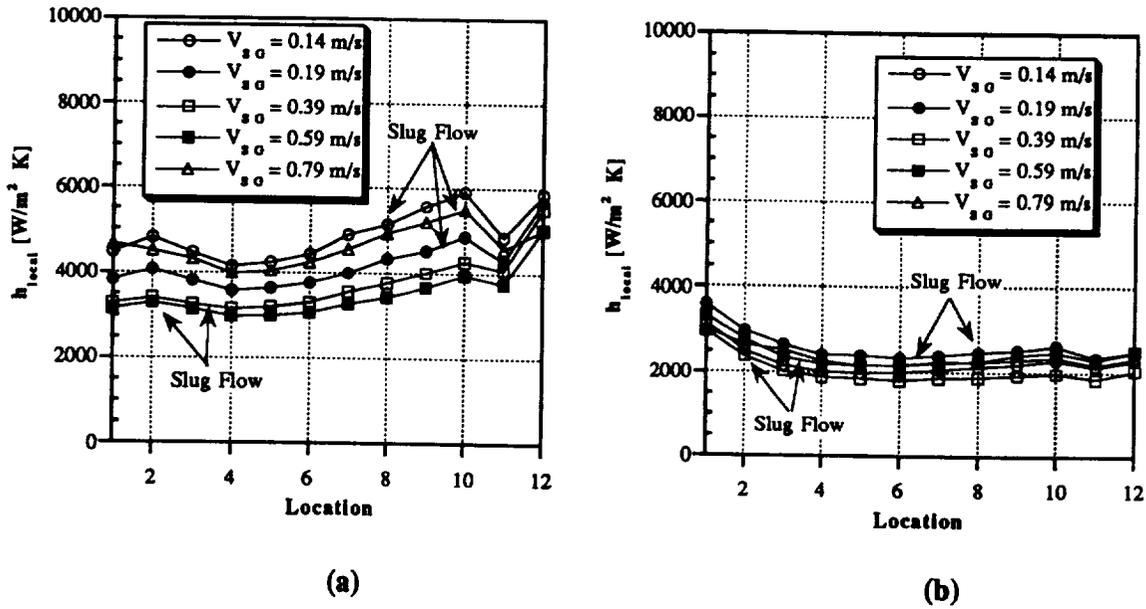**Figure 4. Local Heat Transfer Coefficients at V_{SL}=0.10 m/s; (a) 1-g, (b) μ-g**
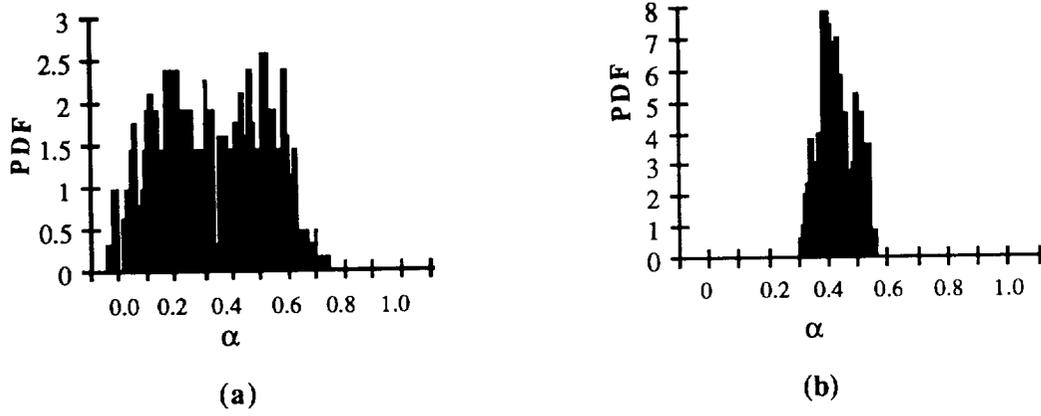
Figure 5. Propability Density Functions for Slug Flow; (a) at 1-g, (b) at μ-g
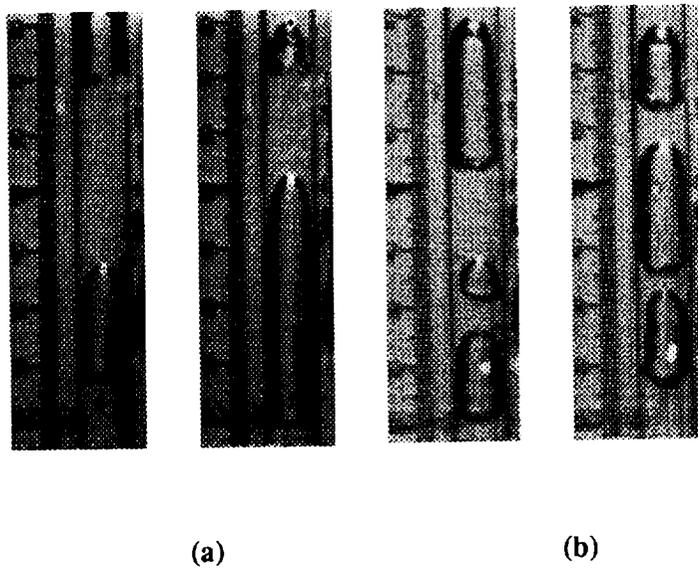

(a)   (b)

Figure 6. Flow Images of Slug flow; (a) at 1-g, (b) at μ-g